processes

MDPI

Article

Radical Copolymerization Kinetics of Bio-Renewable Butyrolactone Monomer in Aqueous Solution

Sharmaine B. Luk and Robin A. Hutchinson *

Department of Chemical Engineering, Queen's University, 19 Division St, Kingston, ON K7L3N6, Canada; sharmaine.luk@queensu.ca

* Correspondence: robin.hutchinson@queensu.ca; Tel.: +1-613-533-3097

Received: 6 September 2017; Accepted: 27 September 2017; Published: 1 October 2017

Abstract: The radical copolymerization kinetics of acrylamide (AM) and the water-soluble monomer sodium 4-hydroxy-4-methyl-2-methylene butanoate (SHMeMB), formed by saponification of the bio-sourced monomer γ-methyl-α-methylene-γ-butyrolactone (MeMBL), are investigated to explain the previously reported slow rates of reaction during synthesis of superabsorbent hydrogels. Limiting conversions were observed to decrease with increased temperature during SHMeMB homopolymerization, suggesting that polymerization rate is limited by depropagation. Comonomer composition drift also increased with temperature, with more AM incorporated into the copolymer due to SHMeMB depropagation. Using previous estimates for the SHMeMB propagation rate coefficient, the conversion profiles were used to estimate rate coefficients for depropagation and termination (k_t). The estimate for $k_{t,SHMeMB}$ was found to be of the same order of magnitude as that recently reported for sodium methacrylate, with the averaged copolymerization termination rate coefficient dominated by the presence of SHMeMB in the system. In addition, it was found that depropagation still controlled the SHMeMB polymerization rate at elevated temperatures in the presence of added salt.

Keywords: bio-renewable; depropagation; ionic strength; parameter estimation

1. Introduction

Water-soluble polymers are used extensively in personal products for hair care [1] and detergents [2], with crosslinked materials utilized as absorbent hydrogels in diapers or feminine products [3]. Other applications include drug delivery [4], flocculation for water recovery in oil sand tailings [5], and metal ion recovery [6]. The bio-derived monomers α-methylene-γ-butyrolactone (MBL) and γ-methyl-α-methylene-γ-butyrolactone (MeMBL) have previously been homopolymerized [7,8] and copolymerized with styrene (ST) and methyl methacrylate (MMA) [9,10], but in bulk or organic solution. Recently, Kollár et al. demonstrated that MBL could be saponified with sodium hydroxide (NaOH) to make a water-soluble monomer, sodium 4-hydroxy-2-methylene butanoate (SHMB), that was copolymerized with acrylamide (AM) and crosslinker to make superabsorbent hydrogels that exhibited superior water absorbency compared to conventional sodium acrylate:AM materials [11]. In an extension of that work, MeMBL was saponified to sodium 4-hydroxy-4-methyl-2-methylene butanoate (SHMeMB) (see Scheme 1), which was copolymerized with AM and crosslinker to make similar superabsorbent materials [12].

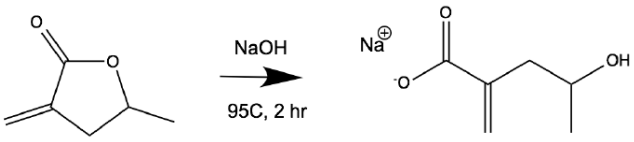

Scheme 1. Saponification of γ-methyl-α-methylene-γ-butyrolactone (MeMBL) using NaOH in water for 2 h at 95 °C to form sodium 4-hydroxy-4-methyl-2-methylene butanoate (SHMeMB).

The SHMeMB:AM hydrogels showed higher water absorbency than SHMB:AM hydrogels, a finding attributed to changes in crosslink density caused by reactivity differences between the two systems [12]. Conversion profiles obtained from in situ NMR showed very slow homopolymerization rates of both SHMB and SHMeMB, and a lowered copolymerization rate for SHMeMB:AM compared to SHMB:AM. The lower reactivity of SHMeMB:AM was partially attributed to differences in the system reactivity ratios, estimated as r_{SHMeMB} = 0.12–0.17 and r_{AM} = 0.95–1.10 for SHMeMB:AM [12] compared to r_{SHMB} = 0.35 ± 0.15 and r_{AM} = 1.42 ± 0.40 for SHMB:AM [11]. Using pulsed-laser polymerization coupled with aqueous-phase size exclusion chromatography (PLP-SEC), the rate of radical chain growth of SHMB:AM copolymers was found to be twice that of SHMeMB:AM under identical conditions. It was not possible, however, to find suitable experimental conditions to directly study SHMeMB homopropagation by the PLP technique. Thus, the copolymerization results were extrapolated to provide the first estimates of the homopropagation rate coefficients (k_p), with very low values of 165 and 25 $L \cdot mol^{-1} \cdot s^{-1}$, estimated at 60 °C in aqueous solution for SHMB and SHMeMB, respectively [12].

As both SHMB and SHMeMB are fully-ionized water-soluble monomers, their polymerization kinetics in aqueous solution are not well-understood. However, previous studies using PLP-SEC, the IUPAC recommended method for determining k_p [13], have examined the radical polymerization behavior of other water-soluble monomers, including non-ionized to fully ionized acrylic and methacrylic acids [14–17] and acrylamide [18]. It is now known that the polymerization kinetics of these monomers in water differ significantly from those of the same monomers in organic solvents, with the k_p values of non-ionized acrylic acid and methacrylic acid significantly higher in water than in methanol and dimethyl sulfoxide (DMSO) [19]. In addition, the kinetics are greatly affected by monomer concentration in aqueous solution, as studied for acrylic acid [16], methacrylic acid [17], and acrylamide [20]. The dependence of k_p on monomer concentration was attributed to the hydrogen-bonding effects between water, monomer, and radical species. Although k_p is dependent on monomer concentration, it was found that the reactivity ratios of AM and non-ionized acrylic acid copolymerization were constant with concentration [21], although the values are dependent on monomer concentration and ionic strength for copolymerization of AM with fully-ionized AA [22,23]. It should be noted that hydrogen-bonding effects are not only present in aqueous solution, but also influence the reactivity ratios of butyl methacrylate (BMA) and 2-hydroxyethyl acrylate (HEA) copolymerization in organic solution, as the relative reactivity of the two monomers is dependent on solvent choice [24].

Another kinetic mechanism important to this study is depropagation. For most radical polymerizations, the monomer addition to a growing macroradical (propagation) can be considered as an irreversible reaction. However, depropagation, the process by which a single monomer unit is released from the growing radical chain, occurs if there is steric hindrance near the radical site. Under these conditions, the propagation and depropagation mechanisms become a reversible reaction pair, with the relative rates (and hence overall rate of polymerization) a function of temperature and monomer concentration. Some monomers that are known to depropagate are BMA [25], itaconates [26], methyl ethacrylate [27], and α-methyl styrene [28], all studied in organic solution. In the presence of appreciable rates of depropagation, the polymerization does not reach full monomer conversion and the reaction can also influence copolymer composition as well as rate, as seen for the radical copolymerization of methyl ethacrylate and styrene (MEA/ST) [29] and BMA/ST at elevated

temperature [25]. It is interesting to note that α-methylene-δ-valerolactone (MVL), a monomer of similar structure to MBL, has been shown to undergo depropagation, with a ceiling temperature of 83 °C [30]. Depropagation of MVL was attributed to its non-planar structure that hinders the radical center, while MBL does not depropagate as it is planar in structure.

In this publication, a series of studies were done to further elucidate the polymerization kinetics of SHMeMB homopolymerization and SHMeMB:AM copolymerization. Polymerizations were conducted at elevated temperatures (60 to 90 °C) to explore the importance of depropagation, using in situ NMR spectroscopy to track monomer conversions. In addition, homopolymerizations were done in the presence of added salt to observe whether the changes in the polymerization rate are similar to those reported for fully ionized acrylic acid (sodium acrylate, NaAA) [31,32] and methacrylic acid (sodium methacrylate, NaMAA) [33]. The homopolymerization conversion profiles were used to estimate the rate coefficients for termination (k_t) and depropagation (k_{dep}), using the parameter estimation capabilities in the PREDICI® software package [34]. Ultimately, the estimated parameters from SHMeMB homopolymerization were implemented in a kinetic model developed to represent SHMeMB:AM copolymerization behavior.

2. Materials and Methods

2.1. Materials

The following chemicals were purchased from Sigma-Aldrich, Canada and used as received: acrylamide (AM, >98%), *N*,*N*′-methylenebis(acrylamide) (BIS, 99%), 2,2′-azobis(2-methyl-propionamidine) dihydrochloride (V-50 initiator, 97%), and sodium hydroxide (NaOH, >97%). 2,2′-Azobis[2-methyl-N-(2-hydroxyethyl)propionamide] (V-86 initiator) was purchased from Wako Pure Chemicals Ltd., USA. Deuterated water (D_2O, 99.8% D) and hydrochloric acid (HCl, 36.5% *w*/*w*) were purchased from Fisher Scientific, Canada and the γ-methyl-α-methylene-γ-butyrolactone (MeMBL, >97%) was provided by DuPont Central Research Laboratories.

2.2. Ring-Opening Saponification of MeMBL

The saponification of MeMBL followed the same procedure as in previous studies [11,12]. For 1 g of MeMBL, 10 mol % excess of NaOH was measured and dissolved in 1 g of D_2O in a small vial with a stir-bar. The saponification reaction took place in an oil bath at 95 °C for 2 h, after which the solution was cooled to room temperature and 1 M HCl was added until a pH of 7 was reached. The SHMeMB mixture was then diluted with D_2O to a final monomer concentration of 40 wt % (including mass of sodium ions). This stock solution was mixed with other components to achieve desired concentrations for the in situ NMR studies. The structure of MeMBL was confirmed by NMR, and ring structures were confirmed to be completely opened to make SHMeMB [12].

2.3. Preparation for In Situ NMR

The in situ NMR method was used to measure the overall monomer conversion profiles, as well as the variation of monomer and polymer composition with conversion, following procedures described by Preusser and Hutchinson [21]. Near-isothermal conditions for the experiments can be assumed based upon the slow rate of polymerization compared to other systems analyzed in the same setup [21]. Copolymerizations were conducted at 3:7 and 4:6 SHMeMB:AM initial molar ratios and 15 wt % monomer concentration in D_2O, with initiator content specified as a weight percent of the total mixture (monomers + D_2O). Homopolymerizations were done at 15 and 30 wt % monomer concentration in D_2O, and salt was added to the monomer mixture relative to the SHMeMB molar amounts. While the preparation of the SHMeMB monomer added slightly to the ionic strength of the solution (addition of 10 mol % excess NaOH followed by neutralization with HCl), this contribution was not considered when reporting salt concentrations in the discussion section.

Overall conversion $X(t)$ was calculated from the decrease in monomer peak integrations relative to the HOD reference peak (residual solvent peak from D_2O at 4.8 ppm), and individual conversions of SHMeMB and AM were used to calculate SHMeMB monomer (f_{SHMeMB}) and polymer mole fractions (F_{SHMeMB}), as detailed in our previous study [12].

2.4. Kinetic Parameters for PREDICI Parameter Estimation

The parameter estimations for SHMeMB homopolymerizations and SHMeMB:AM copolymerizations were done using PREDICI [34], based on the reaction mechanisms listed in Table 1. For SHMeMB:AM copolymerizations, k_t represents an averaged value for all three termination mechanisms; as will be discussed, the values were estimated from individual experimental monomer conversion profiles to provide a perspective on how the averaged rate coefficient varies with monomer composition. As the termination rate is dominated by the large fraction of SHMeMB radicals in the system, the reaction is assumed to occur solely by disproportionation due to their hindered structure; this assumption does not impact the k_t values estimated from the conversion profiles. Depropagation was also considered in the model, based on the assumption that the reaction occurs only if both the penultimate and terminal monomer units of the growing radical chain are SHMeMB, as captured by the probability factor p_{11} [25].

Table 1. Reaction mechanisms for the copolymerization of SHMeMB and acrylamide (AM).

Reaction Mechanisms	
Initiator decomposition	$I \xrightarrow{k_d} 2fR_o^*$
Initiation	$R_0^* + SHMeMB \xrightarrow{k_{p1,1}} SHMeMB_1^*$
	$R_0^* + AM \xrightarrow{k_{p2,2}} AM_1^*$
Propagation	$SHMeMB_n^* + SHMeMB \xrightarrow{k_{p1,1}} SHMeMB_{n+1}^*$
	$SHMeMB_n^* + AM \xrightarrow{k_{p1,2}} AM_{n+1}^*$
	$AM_n^* + SHMeMB \xrightarrow{k_{p2,1}} SHMeMB_{n+1}^*$
	$AM_n^* + AM \xrightarrow{k_{p2,2}} AM_{n+1}^*$
Termination (by disproportionation)	$SHMeMB_n^* + SHMeMB_m^* \xrightarrow{k_t} P_n + P_m$
	$AM_n^* + SHMeMB_m^* \xrightarrow{k_t} P_n + P_m$
	$AM_n^* + AM_m^* \xrightarrow{k_t} P_n + P_m$
Depropagation	$SHMeMB_n^* \xrightarrow{p_{11}k_{dep}} SHMeMB_{n-1}^* + SHMeMB$

The known rate coefficients (initiator decomposition, homopropagation, and reactivity ratios) are shown in Table 2. The initiator efficiency (f) of V-50 was assumed to be 0.8, and for V-86 it was assumed to be 0.38, as determined in a previous study [35]. The propagation rate expression for AM homopolymerization was determined [18] and modelled [20] previously as a function of both monomer concentration and temperature, yielding a $k_{p,AM}$ value of 86,000 $L \cdot mol^{-1} \cdot s^{-1}$ for 15 wt % AM in aqueous solution at 50 °C. Although AM concentration changes with SHMeMB:AM comonomer composition (keeping total monomer content at 15 wt %), the value of $k_{p,AM}$ in the model was kept constant. This assumption is reasonable, as $k_p{}^{cop}$ is dominated by the low value of $k_{p,SHMeMB}$ and not sensitive to small changes in $k_{p,AM}$. As shown in Table S1 in the supporting information, $k_{p,AM}$ values were calculated at a different total AM wt % (while maintaining 15 wt % monomer concentration) and the estimated values for k_t remained the same. The PLP-SEC estimate for $k_{p,SHMeMB}$, obtained at 60 °C and 15 wt % monomer in the previous study [12], was used in this work.

Table 2. Rate expressions for known kinetic coefficients used in model of SHMeMB:AM copolymerization.

Reaction	Rate Expression	References
Decomposition of V-50	$k_d = 9.385 \times 10^{14} \exp(-14{,}890/T(\mathrm{K}))$ $f = 0.8$	[36]
Decomposition of V-86	$k_d = 1.24 \times 10^{13} \exp(-14{,}800/T(\mathrm{K}))$ $f = 0.38$	[35,37]
Propagation of AM	$k_p^0 = 9.5 \times 10^7 \exp(-2189/T(\mathrm{K}))$ $k_p = k_p^0 \exp(-0.01\, c_{AM}(0.0016T + 1.015))$	[18]
Propagation of SHMeMB	$k_p = 25\ \mathrm{L{\cdot}mol^{-1}{\cdot}s^{-1}}$	[12]
Reactivity ratios at 50 °C	$r_{AM} = k_{p2,2}/\ k_{p2,1} = 0.95 \pm 0.01$ $r_{SHMeMB} = k_{p1,1}/\ k_{p1,2} = 0.17 \pm 0.01$	[12]

3. Results and Discussion

3.1. Copolymerization of SHMeMB:AM at Different Temperatures

In the previous study, in situ batch copolymerizations of SHMeMB and AM at 50 °C over a wide range of compositions (initial mole fraction of SHMeMB, f_{SHMeMB}, between 0.1 and 0.8) were used to estimate the reactivity ratios of the system summarized in Table 2. In this work, the study was extended to higher temperatures. Conversion profiles measured for experiments with V-50 initiator at an initial monomer content of 15 wt % and SHMeMB:AM molar ratios of 3:7 (50–80 °C) and 4:6 (50–70 °C) are shown in Figure 1. It is evident that the initial rate of polymerization increases with temperature, as expected due to the accelerated radical production rate as well as the increased k_p values. However, monomer conversion plateaus at less than 100% at the higher temperatures. This limiting conversion does not result from initiator depletion, as 27% of the V-50 remains after 3 h at 70 °C, based on literature values for V-50 decomposition kinetics. The conversion plateau occurs at a lower conversion as the initial fraction of SHMeMB is increased, as seen by comparing the profiles for 3:7 and 4:6 SHMeMB:AM after 3 h. Thus, the presence of SHMeMB not only affects the initial rate of polymerization, but also causes the copolymerization rate to significantly slow down as higher conversions are reached at the higher temperatures.

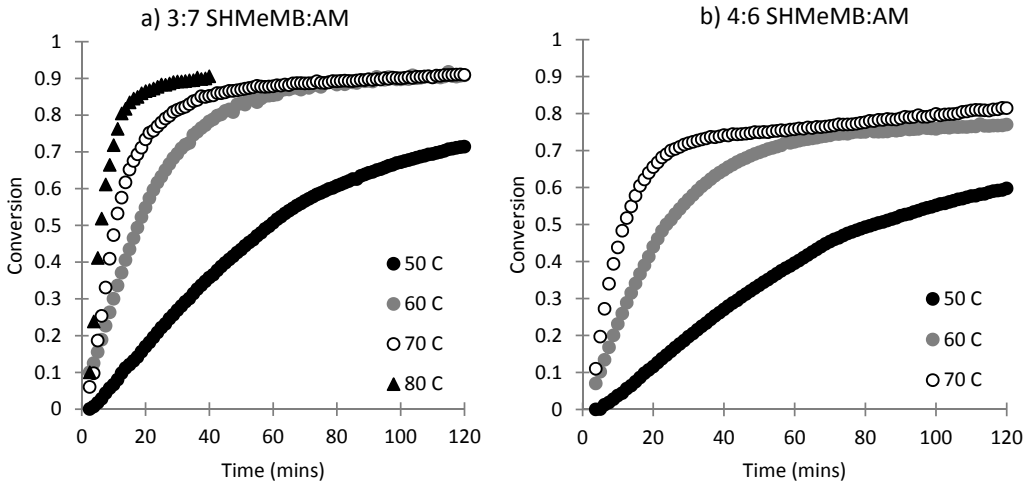

Figure 1. Overall monomer conversion profiles for copolymerizations at (**a**) 3:7 and (**b**) 4:6 initial SHMeMB:AM molar ratios at varying temperatures with 15 wt % monomer and 0.5 wt % V-50.

Individual monomer concentration profiles of SHMeMB and AM at 50, 60, and 70 °C are presented as Figure S1 in the supporting information. The plots show that the rate of SHMeMB consumption becomes very slow at the lowered SHMeMB concentrations reached later in the reactions, while the

consumption of AM continues. This behavior becomes more evident at higher temperatures and increased SHMeMB content, under which conditions the absolute concentration of AM decreases to values below that of SHMeMB, despite its higher initial value. The limiting SHMeMB conversions suggest that depropagation of SHMeMB monomer may be occurring, leading to a significantly decreased rate of polymerization as AM is consumed.

To further explore this possibility, the comonomer composition drifts with conversion at different temperatures are plotted in Figure 2; the curves are normalized by the initial fraction of SHMeMB in the mixture to provide a better comparison by eliminating slight variations in the initial compositions. If SHMeMB depropagation is important, the value of f_{SHMeMB} would increase more significantly with conversion as temperature is increased due to decreased incorporation of SHMeMB under conditions that favour depropagation, as seen in studies of MEA/ST [29] and BMA/ST [25]. As shown in Figure 2, this behavior is indeed observed for the SHMeMB:AM system as temperature increased from 50 to 80 °C. At higher conversions where monomer concentrations are low, the influence of depropagation on SHMeMB consumption becomes more prominent. The reaction temperature was further increased to 90 °C using a different initiator, V-86, as it has a slower rate of decomposition. At 90 °C, there was further deviation of the drift in f_{SHMeMB} with conversion compared to 50 °C. Reactions with V-50 and V-86 were conducted at the same temperatures to verify that composition drift was consistent using both initiators (see Figure S2).

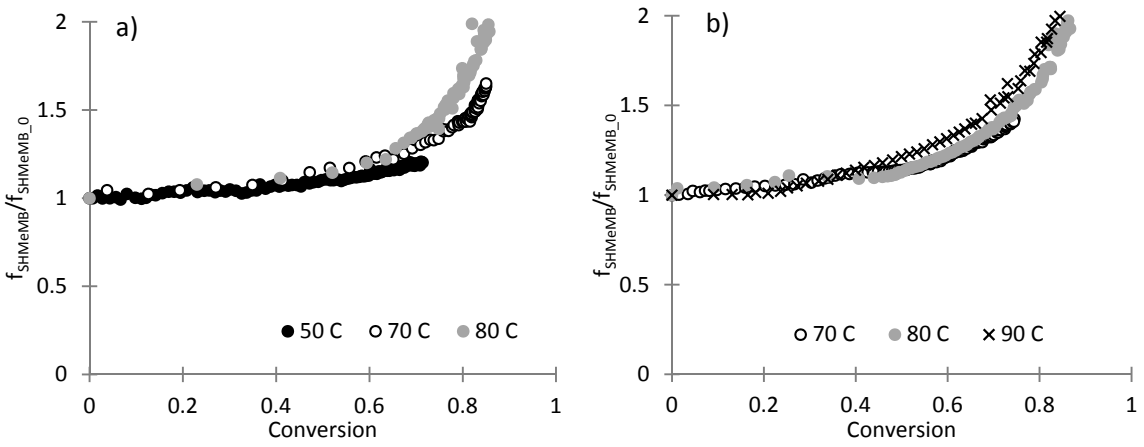

Figure 2. Monomer composition drift with conversion for copolymerization with an initial 3:7 SHMeMB:AM molar ratio, 15 wt % monomer and (**a**) 0.5 wt % V-50 initiator, or (**b**) 1.67 wt % V-86 initiator at varying temperatures (90 °C experiment was conducted with 0.5 wt % V-86). Monomer composition was normalized by initial monomer composition to eliminate the influence of slight variations in the comonomer mixture composition.

As a first step to understanding this behavior, monomer composition drifts measured with 3:7 molar ratio of SHMeMB:AM copolymerizations at 70 and 80 °C were fitted to provide reactivity ratio estimates, with results shown in Figure 3. Two methods were used to fit the experimental data: the first uses the previously determined r_{AM} = 0.951 so that only one parameter (r_{SHMeMB}) was estimated, as depropagation should only influence the addition rate of a SHMeMB monomer to a SHMeMB radical, and thus the effective value of r_{SHMeMB}. For the second fitting, both parameters, r_{AM} and r_{SHMeMB}, were estimated simultaneously.

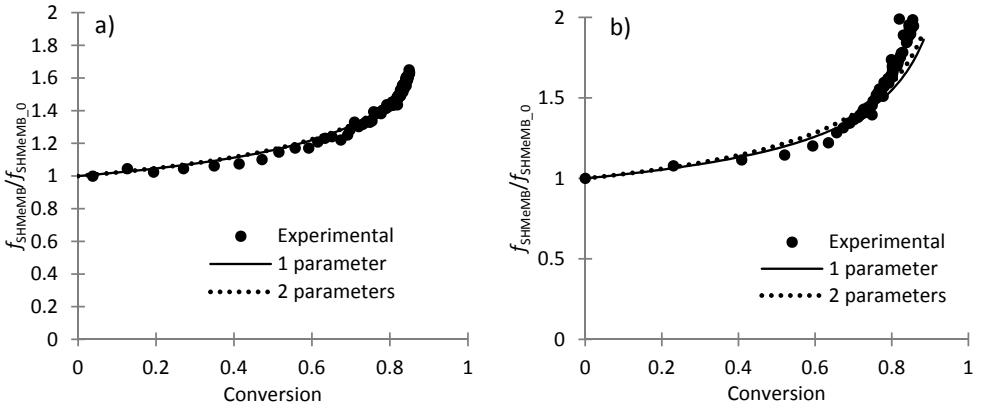

Figure 3. Monomer composition drift for copolymerizations of 3:7 molar ratio of SHMeMB:AM with 15 wt % monomer and 0.5 wt % V-50 at (**a**) 70 and (**b**) 80 °C. The solid line represents parameter estimation with r_{AM} fixed at 0.951 (best-fit value at 50 °C), and the dotted line represents parameter estimation to determine both r_{AM} and r_{SHMeMB}, with values summarized in Table 3.

As shown by Figure 3, both methods gave good representations to the experimental data, but with drastically different estimates for r_{SHMeMB}, as summarized in Table 3. The terminal model reactivity ratio of monomer one (r_1) is defined by Equation (1), where $k_{p,11}$ is the homopropagation rate coefficient for addition of monomer one to a monomer one radical and $k_{p,12}$ is the cross-propagation rate coefficient for the addition of monomer two to a monomer one radical.

$$r_1 = \frac{k_{p,11}}{k_{p,12}} \tag{1}$$

When the value of r_{AM} was fixed at 0.951, the parameter estimation forces r_{SHMeMB} to approach zero, indicating that AM monomer addition is greatly favoured over SHMeMB addition to a SHMeMB terminal radical. Estimating r_{SHMeMB} and r_{AM} simultaneously at 70 °C gave an r_{AM} value that was close to the value determined at 50 °C, and lowered the r_{SHMeMB} value to 0.120 (from 0.169 at 50 °C). At 80 °C, r_{SHMeMB} decreased to an even lower value of 0.046 due to more prominent depropagation effects at higher temperatures. While these values seem plausible, the uncertainty in the estimates are large. Nonetheless, they are consistent with the expectations of depropagation.

Table 3. Reactivity ratios estimates from copolymerization of 3:7 molar ratio of SHMeMB:AM with 15 wt % monomer and 0.5 wt % V-50 at 70 and 80 °C. The "one parameter" method estimates r_{SHMeMB} with r_{AM} fixed at 0.951, and the "two parameter" method estimates both r_{AM} and r_{SHMeMB}.

	70 °C		**80 °C**	
	1 Parameter	**2 Parameters**	**1 Parameter**	**2 Parameters**
r_{SHMeMB}	0.005 ± 0.008	0.12 ± 0.22	$7 \times 10^{-6} \pm 7 \times 10^{-3}$	0.05 ± 0.17
r_{AM}	-	1.04 ± 0.17	-	1.06 ± 0.21

It is important to note that the parameter estimation fits the reactivity ratios based on the terminal model (i.e., no depropagation), assuming that the value of $k_{p,SHMeMB}$ remains constant with conversion. In the case of depropagation, the $k_{p,11}$ value should be considered as an effective value, $k_p{}^{eff}$, dependent on k_p, k_{dep} and monomer concentration [M] as shown in Equation (2) [26], such that r_{SHMeMB} would change with conversion.

$$k_p^{eff} = k_p - \frac{k_{dep}}{[M]} \tag{2}$$

Thus, the conversion profiles for SHMeMB homopolymerizations are first used to estimate k_{dep} before returning to analysis of the copolymerization system.

3.2. Homopolymerization Kinetics of SHMeMB

To investigate depropagation kinetics further, the in situ NMR technique was used to study homopolymerization of SHMeMB at increased temperature and initiator content (75 °C and 1 wt % V-86), with reaction times (14 h) considerably extended compared to copolymerizations. The conversion profiles, shown in Figure 4, were the same for both initial monomer concentrations (15 and 30 wt %), consistent with reports that monomer concentration did not have a large effect on k_p for other fully ionized monomers such as NaMAA [17]. However, no difference in the final conversions is seen between the two experiments, indicating that monomer concentrations were not yet approaching the equilibrium values at which depropagation would cause a difference in limiting conversion.

The possible effects of depropagation on the homopolymerization of SHMeMB were investigated at higher temperatures. In Figure 4, the initial rate of polymerization is seen to be faster at 90 °C than at 75 °C as expected, but the rate eventually slows down such that the final conversion reached is lower than at 75 °C. The decrease in polymerization rate at 90 °C is not due to the lack of initiator, as there is still 25% remaining after 16 h [37]. Thus, the conversion profiles support the hypothesis that depropagation is affecting SHMeMB polymerization, consistent with the observation of increased AM incorporation into the SHMeMB:AM copolymer observed at elevated temperatures.

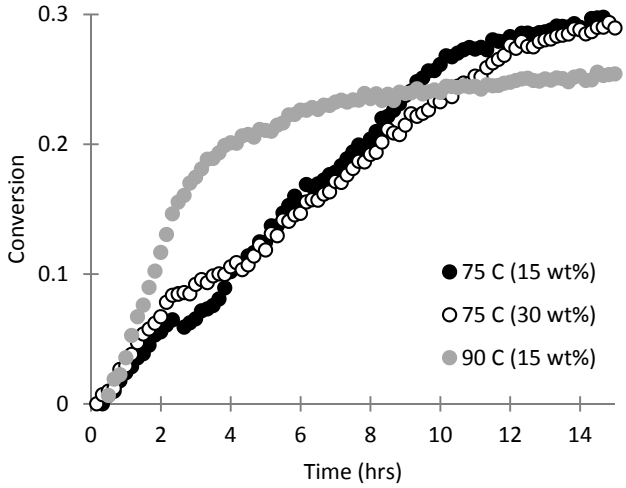

Figure 4. Monomer conversion profiles obtained by homopolymerization of SHMeMB at 15 and 30 wt % at 75 °C and 1 wt % V-86, and at 15 wt % and 90 °C.

It was previously demonstrated that the polymerization rate of fully ionized acrylic acid was influenced by the addition of a salt, such that at a molar ratio of 1:5.7 [AA^-]:[NaCl] the polymerization rate of fully ionized AA (NaAA) was comparable to that of non-ionized AA [31]. It was proposed that the screening of charges by the added salt reduced the repulsion between the ionized monomers and ionized radical sites, therefore enhancing the polymerization rate of fully-ionized AA. Thus, NaCl was added to SHMeMB homopolymerizations to examine for a similar effect, as shown in Figure 5. The polymerization rate at 75 °C was found to decrease with added salt, with the rate of polymerization perhaps slightly lower at the 1:1 ratio of SHMeMB]:[NaCl] compared to the 1:0.5 ratio.

Although the rate of monomer conversion of NaAA was increased by increasing ionic strength [31], a similar increase was not observed for NaMAA [17]. However, a separate study showed that the k_p of NaMAA did increase with ionic strength [32]. Therefore, it can be concluded that k_p and k_t for ionized monomers are both affected (increased) by the presence of salt, but to different extents, according to the monomer. Individual estimates are not available for SHMeMB, but the conversion profiles in Figure 5a indicate that k_t is enhanced in the presence of NaCl to a greater extent than k_p, hence decreasing the overall rate of polymerization at 75 °C. As shown in Figure 5b, the addition of NaCl to the polymerization at 90 °C, however, has no effect on the conversion profile. Depropagation

is more important at this elevated temperature, complicating the situation; however, the net effect of the added salt on the rate of conversion is minor.

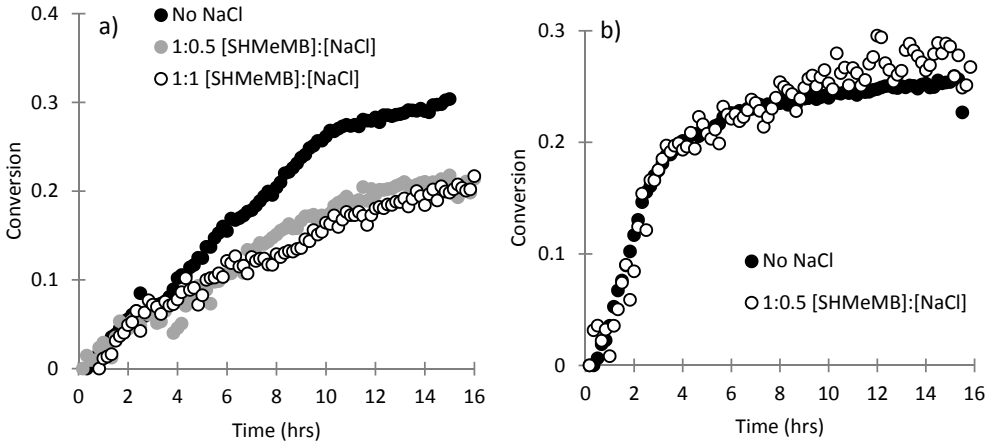

Figure 5. Monomer conversion profiles obtained from homopolymerizations of SHMeMB at 15 wt % with (**a**) added NaCl salt at 75 °C and 1 wt % V-86, and (**b**) at 90 °C with added NaCl at 1:0.5 [SHMeMB]:[NaCl] molar ratio.

3.3. Parameter Estimation for SHMeMB Homopolymerizations

The SHMeMB homopolymerization conversion profiles presented in Section 3.2 are used in this section to estimate both the termination (k_t) and depropagation (k_{dep}) coefficients using the data-fitting tools in PREDICI based on the mechanisms shown in Table 1 (initiation, propagation, depropagation and termination). As conversion profiles are a function of the ratios of rate coefficients (k_{dep}/k_p and $k_p/k_t^{0.5}$), the strategy employed was to use the previously-estimated propagation coefficient (k_p) of SHMeMB from the PLP-SEC study [12], and to estimate k_{dep} simultaneously with k_t. For simplicity, the k_p value of 25 L·mol^{-1}·s^{-1} estimated at 60 °C was used, as the activation energy for propagation is not known. Thus, the estimates for k_t and k_{dep} at 75 and 90 °C are lower than the true values, but could be corrected once the temperature dependency of k_p is determined.

The initial fitting of the SHMeMB homopolymerizations curves, shown in Figure 6, was conducted assuming no depropagation occurs (k_{dep} = 0). The model fits the experimental data reasonably well at 75 °C until the point at which the rate of polymerization seemed to decrease, around 10 h into the reaction. However, it is evident that the model with no depropagation was not sufficient in fitting the experiment conversion profile at 90 °C, predicting a continued increase in conversion not observed experimentally. The best fit value of k_t is 1.3 × 10^6 L·mol^{-1}·s^{-1} at both 75 and 90 °C, although the true values would be lower (due to the assumption that depropagation does not occur). Furthermore, k_t does not seem to be a large function of temperature, as the same value was able to fit the initial polymerization rate for both 75 and 90 °C. These estimates of k_t are higher than recently reported values for NaAA of ~10^5 L·mol^{-1}·s^{-1} [38].

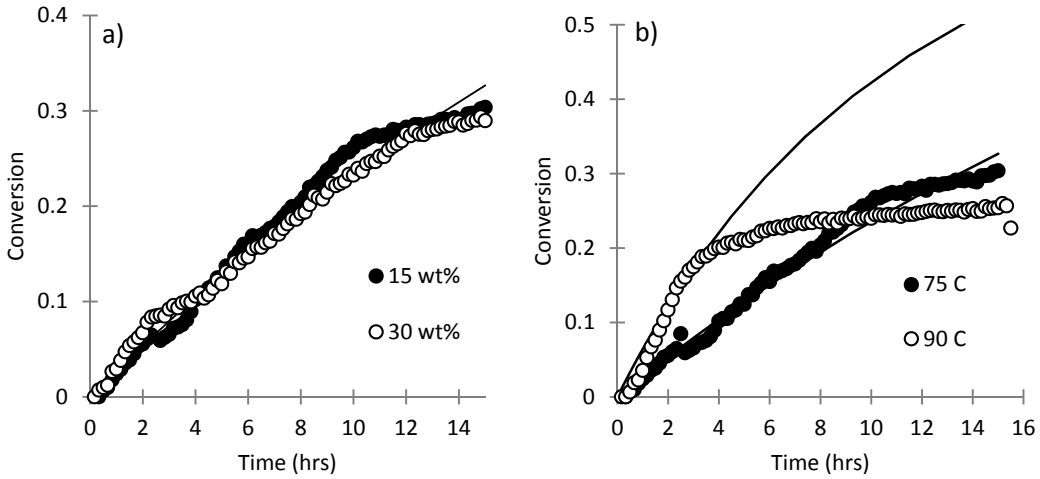

Figure 6. Fit of the homopolymerization SHMeMB model assuming no depropagation to monomer conversion profiles obtained at (**a**) 75 °C with 1 wt % V-86 at different monomer concentrations, and (**b**) at different temperatures with 1 wt % V-86 and 15 wt % monomer. Solid lines represent model output, with experimental results indicated by data points.

The experimental conversion profile of SHMeMB hompolymerization at 75 °C was converted using the integrated conversion equation for a batch isothermal reaction, Equation (3), to generate a $k_p/k_t^{0.5}$ vs. conversion plot. In Equation (3), X represents conversion, k_d is the decomposition rate coefficient of V-86 initiator, t is reaction time, $[I]_0$ is initial initiator concentration, and f is initiator efficiency.

$$\frac{k_p}{k_t^{0.5}} = \frac{ln(1-X)}{exp(0.5k_dt)-1}\sqrt{\frac{k_d}{8[I]_0 f}} \quad (3)$$

Note that Equation (3) is derived assuming that both k_p and k_t are constant with conversion, and that depropagation does not occur in the system. In general, the $k_p/k_t^{0.5}$ ratio calculated from the experimental data at 75 °C, as shown in Figure 7, is fairly constant until it reaches a conversion of 25%, at which point it starts to decrease, likely due to the influence of depropagation. (The $k_p/k_t^{0.5}$ values at <10% conversion were omitted due to scatter of experimental data in the initial stages of the reaction.) Assuming that depropagation was negligible between 0 and 25% conversion and a k_p value of 25 L·mol^{-1}·s^{-1}, the average value of $k_p/k_t^{0.5}$ of 0.022 (L·mol^{-1}·s^{-1})$^{0.5}$ in this region is used to estimate a value of k_t of 1.30 × 10^6 L·mol^{-1}·s^{-1}, in agreement with the value fit to generate the conversion profiles in Figure 6. Also in agreement with Figure 6, the $k_p/k_t^{0.5}$ ratio begins to decrease at a lower conversion at 90 °C, leading to the overestimation of the reaction rate without the consideration of depropagation.

The k_t value of 1.30 × 10^6 L·mol^{-1}·s^{-1} was estimated using the $k_p/k_t^{0.5}$ equation assuming depropagation was negligible in the early stages of the reaction, but the true extent of depropagation is still unknown at 75 and 90 °C. Using parameter estimation on PREDICI, both k_t and k_{dep} values were simultaneously estimated to be 1.4 ± 1.8 × 10^5 L·mol^{-1}·s^{-1} and 21 ± 6 s^{-1}, respectively, at 75 °C. The estimated value k_t is an order of magnitude lower than estimated using the $k_p/k_t^{0.5}$ plot, but is in reasonable agreement with reported estimates for other ionized monomers [33]. However, the 95% confidence interval encompasses zero, due to the difficulty in estimating both k_t and k_{dep} from a single conversion profile. Thus, the strategy taken was to fix k_t at the value of 1.4 × 10^5 L·mol^{-1}·s^{-1}, and estimate only the k_{dep} values from the conversion profiles obtained with 15 wt % SHMeMB at both 75 and 90 °C. The resulting fits to the conversion profiles are shown in Figure 8, with best fit values for k_{dep} of 20.9 ± 0.6 and 26.8 ± 0.4 s^{-1} at 75 and 90 °C, respectively. The best fit profiles are compared to the curves generated assuming no depropagation (at 75 °C extended to longer time), to further

illustrate that the higher k_t value estimated from the $k_p/k_t^{0.5}$ plot did not adequately represent the shape of the curve. Although the estimation at 90 °C did not fit as well to the experimental data, the higher estimated value of k_{dep} indicates that, as expected, depropagation is enhanced at elevated temperatures. Furthermore, the fitting indicates an SHMeMB ceiling temperature (at a standard state of 1 mol·L^{-1}) of about 90 °C, at which point k_p and k_{dep} estimates are almost identical. It is interesting to note that this value is close to the ceiling temperature of 83 °C reported for MVL [30], although the latter was polymerized in a closed ring form in organic solvent.

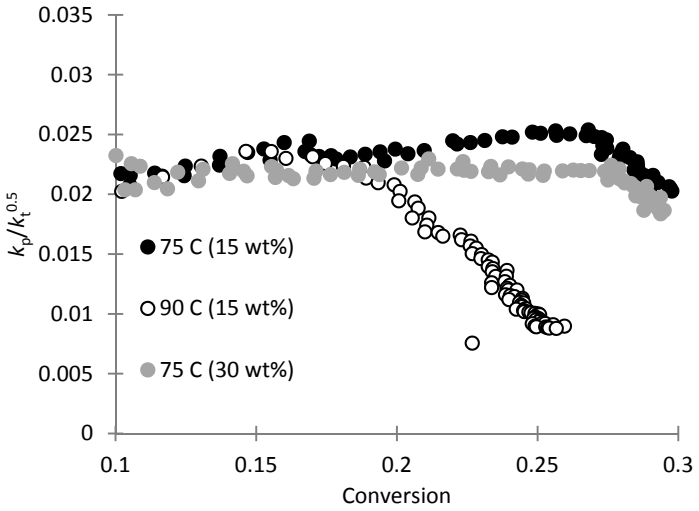

Figure 7. $k_p/k_t^{0.5}$ vs. conversion profile of SHMeMB homopolymerization at 75 °C with 15 and 30 wt % monomer concentration and at 90 °C with 15 wt % monomer and 1 wt % V-86 for 15 h.

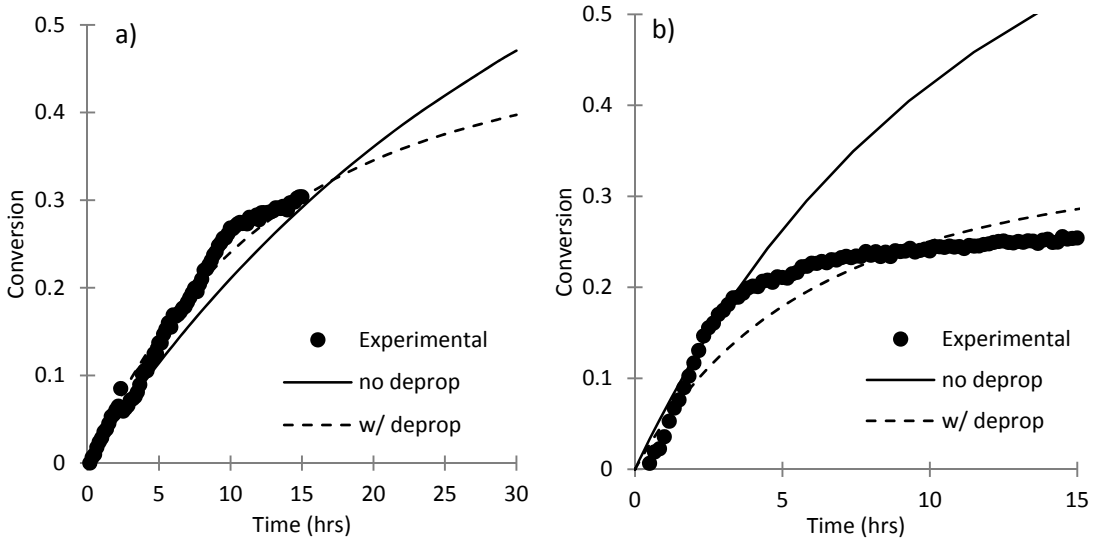

Figure 8. Conversion profile of SHMeMB homopolymerization with 15 wt % monomer and 1 wt % V-86 at (**a**) 75 °C and (**b**) at 90 °C. Lines indicate best-fit simulation results with (- - - -) and without (——) depropagation.

Termination and depropagation rate coefficients were also estimated at the higher monomer concentration conditions of 30 wt % SHMeMB at 75 °C with 1 wt % V-86. From previous PLP-SEC studies [39], k_p^{cop} of 10 mol % SHMeMB in SHMeMB:AM mixtures at 10 and 20 wt % were within experimental error. Therefore, a k_p value of 25 L·mol^{-1}·s^{-1} was also assumed for SHMeMB homopolymerization at 30 wt %. The value of k_{dep} was also kept constant, and the conversion profile

used to estimate a k_t value of 6.15 ± 0.02 × 10^5 L·mol^{-1}·s^{-1}, with the fitted curve compared to the experimental conversion profile in Figure 9. Even though the observed conversion profiles at 15 and 30 wt % were nearly identical, the estimated values for k_t increased significantly, a finding consistent with a previous study that showed that the k_t of fully ionized NaMAA increased with monomer concentration [40].

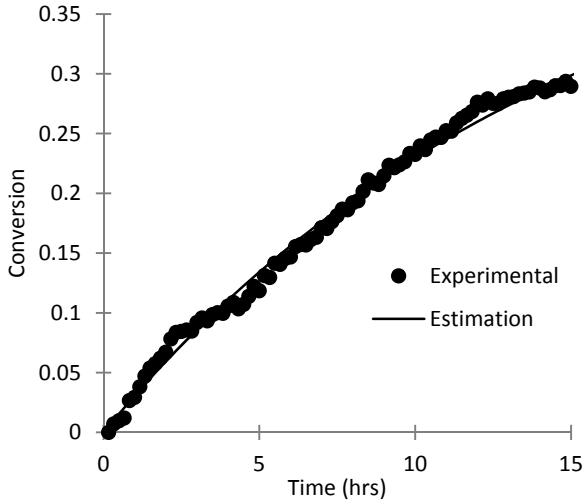

Figure 9. Monomer conversion profiles for the homopolymerization of SHMeMB at 75 °C with 1 wt % V-86 and 30 wt % monomer. The solid line represents the estimated conversion profile using parameter estimation.

Finally, parameter estimations were also done for the homopolymerizations of SHMeMB with added NaCl at 75 °C. While depropagation is generally attributed to the steric hindrance near the α-carbon, it is possible that electrostatic repulsion from the ionized carboxylic groups can also affect the mechanism. Nonetheless, it was assumed that k_{dep} remains the same with added salt (21 s^{-1} as determined previously), as the first order depropagation mechanism is less likely to be influenced by the reaction environment than the bimolecular termination and propagation reactions and, as previously stated, both the k_p and k_t values for polymerizations of fully ionized monomers with added salt have been observed to increase with ionic strength [32]. The estimated conversion profiles are compared to the experimental results in Figure 10. As expected, the estimated values for k_p and k_t summarized in Table 4 have high uncertainty due to the difficulty of estimating two rate coefficients from the same conversion profile, with 95% confidence intervals encompassing zero. However, the best fit values are roughly the same for both 1:0.5 and 1:1 molar ratios of [SHMeMB]:[NaCl]. While the estimated values for k_p did not increase greatly with the addition of salt (from 25 to ~30 L·mol^{-1}·s^{-1}), the estimates for the k_t values increased an order of magnitude to 1 × 10^6 L·mol^{-1}·s^{-1}, significantly larger than the value of 1 × 10^5 L·mol^{-1}·s^{-1} estimated without salt. Although estimated with high uncertainty, it is interesting to note that this increase in k_t is consistent with the increase estimated for the 30 wt % SHMeMB homopolymerization, suggesting that charge screening provided from either the higher SHMeMB monomer concentration or added salt lowers the electrostatic barrier to radical–radical termination.

Table 4. Estimated values for k_p and k_t for homopolymerizations of SHMeMB with added salt at 75 °C with 1 wt % V-86 and 15 wt % monomer assuming a k_{dep} value of 21 s^{-1}. Results are shown for reactions done with 1:0.5 and 1:1 molar ratios of [SHMeMB]:[NaCl].

	1:0.5 [SHMeMB]:[NaCl]		1:1 [SHMeMB]:[NaCl]	
		95% Confidence		95% Confidence
k_p ($L \cdot mol^{-1} \cdot s^{-1}$)	30.3	±50.9	29.2	±37.0
k_t ($L \cdot mol^{-1} \cdot s^{-1}$)	9.98×10^5	$\pm 7.96 \times 10^6$	1.01×10^6	$\pm 6.32 \times 10^6$

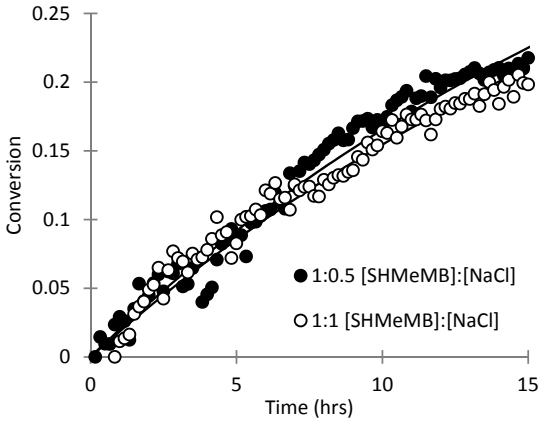

Figure 10. Monomer conversion profiles from homopolymerization of SHMeMB with different concentrations of added NaCl salt at 75 °C with 1 wt % V-86 and 15 wt % monomer. The solid lines represent the simulated conversion profiles using parameter estimation.

To summarize, despite considerable uncertainty in the parameter estimations, the analysis of the SHMeMB homopolymerization conversion profiles suggests that the system is characterized by similar k_t values to other ionized monomers, but has very low propagation rates and significant depropagation. A large increase in k_t was required to fit the conversion profiles measured with added salt and with increased monomer concentration, consistent with trends observed in NaMAA [40].

3.4. Parameter Estimation for SHMeMB:AM Copolymerizations with Depropagation

The knowledge gained regarding the kinetic behavior of SHMeMB is here applied to the interpretation of the experimental SHMeMB:AM copolymerizations. Details of the PREDICI model, which assumes terminal chain-growth kinetics and SHMeMB depropagation, and uses a single k_t value to represent termination in the two-monomer system, is presented in Section 2.4. Using the coefficients at 50 °C summarized in Table 2, and a SHMeMB k_{dep} value of 21 s^{-1}, k_t, values of the copolymerization system were estimated at 50 °C for the different molar ratios of SHMeMB and AM studied experimentally. The estimated k_t values of SHMeMB:AM copolymers are plotted as a function of f_{SHMeMB} in Figure 11, with $k_{t,AM}$ and $k_{t,SHMeMB}$ included for reference. The termination rate coefficient for AM ($k_{t,AM}$) was reported as a function of monomer concentration and temperature [20,41]. At 50 °C, $k_{t,AM}$ values at 10 and 20 wt % were calculated to be 5.2×10^8 and 4.2×10^8 $L \cdot mol^{-1} \cdot s^{-1}$, respectively. Taking the average of the two values gave an estimate of $k_{t,AM}$ of 4.7×10^8 $L \cdot mol^{-1} \cdot s^{-1}$ for 15 wt % monomer, several orders of magnitude higher than the k_t of SHMeMB ($k_{t,SHMeMB}$) estimated as 1.4×10^5 $L \cdot mol^{-1} \cdot s^{-1}$ at 15 wt % and 75 °C in Section 3.4. The fitting of k_t to the SHMeMB:AM copolymerizations at 50 °C with 0.5 wt % V-50 and 15 wt % monomer provided a very good representation of the experimental conversion profiles, as seen in Figure S3.

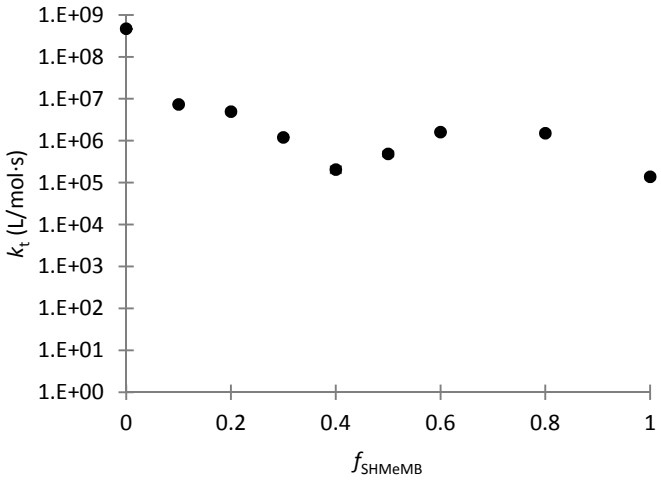

Figure 11. k_t of SHMeMB:AM copolymers estimated for copolymerizations done at 50 °C with 0.5 wt % V-50 and 15 wt % monomer.

Figure 11 shows an immediate drop of two orders of magnitude upon addition of SHMeMB as a comonomer to AM, with values further decreasing to ~10^5 L·mol^{-1}·s^{-1} as f_{SHMeMB} increases to 0.4, at which point the estimates level out. The value of 10^5 L·mol^{-1}·s^{-1} is similar to the estimated value for $k_{t,SHMeMB}$ in the previous section, and also the value of 3.6 × 10^5 L·mol^{-1}·s^{-1} reported for homotermination of NaAA at 20 wt % and 50 °C in aqueous solution [38]. Comparable k_t values for SHMeMB and NaAA indicate that the slow termination of two radicals in these systems is dominated by the electrostatic repulsion of the charged species near the radical site, rather than the steric hindrance that leads to the slow propagation and occurrence of depropagation of SHMeMB.

The k_t value estimated for the copolymerization is an averaged value that describes all termination events in the SHMeMB:AM copolymerization, assuming terminal model kinetics. This averaging is described by Equation (4), where $f_{r,SHMeMB}$ is the fraction of SHMeMB terminal radicals, $f_{r,AM}$ is the fraction of AM terminal radicals, and $k_{t,SA}$ is the rate coefficient describing the cross-termination of SHMeMB and AM radicals [28].

$$k_t = k_{t,SHMeMB} f_{r,SHMeMB}^2 + 2k_{t,SA} f_{r,SHMeMB} f_{r,AM} + k_{t,AM} f_{r,AM}^2 \quad (4)$$

According to Equation (4), k_t must be dominated by the value of $k_{t,SHMeMB}$, as its value decreases by two orders of magnitude from the value of $k_{t,AM}$ when only 10 mol % of SHMeMB is added to the mixture. This large drop indicates that even at a low initial SHMeMB monomer fraction, the fraction of SHMeMB radicals ($f_{r,SHMeMB}$) is very high. Indeed, given the reactivity ratios of the system and the high homopropagation rate of AM (see Table 2), it can be calculated that at f_{SHMeMB} = 0.1, $f_{r,SHMeMB}$ is greater than 99%, such that SHMeMB-SHMeMB termination is the dominant termination event.

4. Conclusions

The difference in reactivity between SHMeMB and SHMB [12] motivated these further kinetic studies to explore the effects of depropagation and added salt on the polymerization rate. A plateau in conversion was observed for SHMeMB:AM copolymerizations conducted at 3:7 and 4:6 molar ratios and elevated temperatures, with monomer composition drift occurring at a faster rate as temperature increased and AM incorporated faster as SHMeMB units became more prone to depropagation. Homopolymerizations of SHMeMB at 75 and 90 °C provided further evidence of depropagation, as conversion reached a lowered equilibrium value at the higher temperature. Upon the addition of salt, the SHMeMB homopolymerization rate decreased at 75 °C, but not at 90 °C, due to the dominating effect of depropagation over the screening of charges provided by counterions.

The experimental data was fitted to models developed in PREDICI in order to estimate termination (k_t) and depropagation (k_{dep}) rate coefficients for SHMeMB, assuming a constant k_p value of 25 L·mol^{-1}·s^{-1}. The k_t values were estimated to be ~10^5 L·mol^{-1}·s^{-1}, similar in magnitude to those reported for NaAA [38] and NaMAA [33], and a ceiling temperature of ~90 °C was estimated. While these estimates have considerable uncertainty, the modeling effort has provided some valuable insights into the polymerization behavior of the system. The finding that $k_{t,SHMeMB}$ is of similar magnitude to other ionic monomers indicates that electrostatic repulsion of charged radical species, rather than steric hindrance from bulky substituents, is the reason for slow termination. The addition of salt and increase in monomer concentration both increased k_p but had a greater effect on the estimated values of k_t, showing that addition of salt had a similar effect to an increased concentration of ionized monomers on the polymerization rate. The knowledge gathered from parameter estimations were then implemented to estimate k_t values for SHMeMB:AM copolymerizations, which were found to be much lower than the known value of 10^8 L·mol^{-1}·s^{-1} for $k_{t,AM}$ but similar in magnitude to the estimates of $k_{t,SHMeMB}$. This result suggests that k_t in the SHMeMB:AM copolymerization system is largely dominated by $k_{t,SHMeMB}$ because of the large fraction of charged SHMeMB radicals.

Supplementary Materials: The table and additional figures discussed in the text are available online at www.mdpi.com/2227-9717/5/4/55/s1.

Acknowledgments: The authors would like to thank the Natural Science and Engineering Research Council for their financial support.

Author Contributions: SBL and RAH conceived and designed the experiments; SBL performed the experiments and analyzed the results; SBL and RAH developed the model; SBL performed the parameter estimation; and SBL and RAH wrote the paper.

Conflicts of Interest: The authors declare no conflict of interest.

References

1. Syed, N.; Habib, W.W.; Kuhajda, A.M. Water-Soluble Polymers in Hair Care. In *Water Soluble Polymers*; Springer: Boston, MA, USA, 2002; pp. 231–244. ISBN 978-0-306-46915-2.
2. Hayashi, Y.; Lu, D.; Kobayashi, N. Application of Ultra-High Molecular Weight Amphoteric Acrylamide Copolymers to Detergents. In *Water Soluble Polymers*; Springer: Boston, MA, USA, 2002; pp. 245–250. ISBN 978-0-306-46915-2.
3. Ahmed, E.M. Hydrogel: Preparation, characterization, and applications: A review. *J. Adv. Res.* **2015**, *6*, 105–121. [CrossRef] [PubMed]
4. Kadajji, V.; Betageri, G. Water Soluble Polymers for Pharmaceutical Applications. *Polymers* **2011**, *3*, 1972–2009. [CrossRef]
5. Vedoy, D.; Soares, J. Water-soluble polymers for oil sands tailing treatment: A Review. *Can. J. Chem. Eng.* **2015**, *93*, 888–904. [CrossRef]
6. Rivas, B.L.; Pereira, E.; Palencia, M.; Sánchez, J. Water-soluble functional polymers in conjunction with membranes to remove pollutant ions from aqueous solutions. *Prog. Polm. Sci.* **2011**, *36*, 294–322. [CrossRef]
7. Akkapeddi, M.K. Poly(α-methylene-γ-butyrolactone) Synthesis Configurational Structure, and Properties. *Macromolecules* **1979**, *12*, 546–551. [CrossRef]
8. Suenaga, J.; Sutherlin, D.M.; Stille, J. Polymerization of (RS)-and (R)-a-Methylene-y-methyl-y-butyrolactone. *Macromolecules* **1984**, *17*, 2913–2916. [CrossRef]
9. Ueda, M.; Takahashi, M. Radical-initiated homo- and copolymerization of α-methylene-γ-butyrolactone. *J. Polym. Sci.* **1982**, *20*, 2819–2828. [CrossRef]
10. Cockburn, R.A.; McKenna, T.F.; Hutchinson, R.A. An Investigation of Free Radical Copolymerization Kinetics of the Bio-renewable Monomer γ-Methyl-α-methylene-γ-butyrolactone with Methyl methacrylate and Styrene. *Macromol. Chem. Phys.* **2010**, *211*, 501–509. [CrossRef]
11. Kollár, J.; Mrlík, M.; Moravčíková, D.; Kroneková, Z.; Liptaj, T.; Lacík, I.; Mosnáček, J. Tulips: A Renewable Source of Monomer for Superabsorbent Hydrogels. *Macromolecules* **2016**, *49*, 4047–4056. [CrossRef]
12. Luk, S.B.; Kollár, J.; Chovancová, A.; Mrlík, M.; Lacík, I.; Mosnáček, J.; Hutchinson, R.A. Superabsorbent hydrogels made from bio-derived butyrolactone monomers in aqueous solution. *Polym. Chem.* 2017. [CrossRef]

13. Buback, M.; Gilbert, R.G.; Russell, G.T.; Hill, D.J.T.; Moad, G.; O'Driscoll, K.F.; Shen, J.; Winnik, M.A. Consistent values of rate parameters in free radical polymerization systems. II. Outstanding dilemmas and recommendations. *J. Polym. Sci. Part A Polym. Chem.* **1992**, *30*, 851–863. [CrossRef]
14. Beuermann, S.; Buback, M.; Hesse, P.; Lacík, I. Free-Radical Propagation Rate Coefficient of Nonionized Methacrylic Acid in Aqueous Solution from Low Monomer Concentrations to Bulk Polymerization. *Macromolecules* **2006**, *39*, 184–193. [CrossRef]
15. Lacík, I.; Beuermann, S.; Buback, M. PLP-SEC Study into Free-Radical Propagation Rate of Nonionized Acrylic Acid in Aqueous Solution. *Macromolecules* **2003**, *36*, 9355–9363. [CrossRef]
16. Lacík, I.; Beuermann, S.; Buback, M. PLP-SEC Study into the Free-Radical Propagation Rate Coefficients of Partially and Fully Ionized Acrylic Acid in Aqueous Solution. *Macromol. Chem. Phys.* **2004**, *205*, 1080–1087. [CrossRef]
17. Lacík, I.; Učňová, L.; Kukučková, S.; Buback, M.; Hesse, P.; Beuermann, S. Propagation Rate Coefficient of Free-Radical Polymerization of Partially and Fully Ionized Methacrylic Acid in Aqueous Solution. *Macromolecules* **2009**, *42*, 7753–7761. [CrossRef]
18. Lacík, I.; Chovancová, A.; Uhelska, L.; Preusser, C.; Hutchinson, R.A.; Buback, M. PLP-SEC Studies into the Propagation Rate Coefficient of Acrylamide Radical Polymerization in Aqueous Solution. *Macromolecules* **2016**, *49*, 3244–3253. [CrossRef]
19. Kuchta, F.D.; van Herk, A.M.; German, A.L. Propagation Kinetics of Acrylic and Methacrylic Acid in Water and Organic Solvents Studied by Pulsed-Laser Polymerization. *Macromolecules* **2000**, *33*, 3641–3649. [CrossRef]
20. Preusser, C.; Chovancová, A.; Lacík, I.; Hutchinson, R.A. Modeling the Radical Batch Homopolymerization of Acrylamide and Aqueous Solution. *Macromol. React. Eng.* **2016**, *10*, 490–501. [CrossRef]
21. Preusser, C.; Hutchinson, R.A. An In Situ NMR Study of Radical Copolymerization Kinetics of Acrylamide and Non-Ionized Acrylic Acid in Aqueous Solution. *Macromol. Symp.* **2013**, *333*, 122–137. [CrossRef]
22. Preusser, C.; Ezenwajiaku, I.H.; Hutchinson, R.A. The Combined Influence of Monomer Concentration and Ionization on Acrylamide/Acrylic acid Composition in Aqueous Solution Radical Batch Copolymerization. *Macromolecules* **2016**, *49*, 4746–4756. [CrossRef]
23. Riahinezhad, M.; McManus, N.; Penlidis, A. Effect of Monomer Concentration and pH on Reaction Kinetics and Copolymer Microsctructure of Acrylamide/Acrylic Acid Copolymer. *Macromol. React. Eng.* **2015**, *9*, 100–113. [CrossRef]
24. Schier, J.E.; Hutchinson, R.A. The influence of hydrogen bonding on radical chain-growth parameters for butyl methacrylate/2-hydroxyethyl acrylate solution copolymerization. *Polym. Chem.* **2016**, *7*, 4567–4574. [CrossRef]
25. Li, D.; Li, N.; Hutchinson, R.A. High-Temperature Free Radical Copolymerization of Styrene and Butyl Methacrylate with Depropagation and Penultimate Kinetics Effects. *Macromolecules* **2006**, *39*, 4366–4373. [CrossRef]
26. Szablan, Z.; Stenzel, M.H.; Davis, T.P.; Barner, L.; Barner-Kowollik, C. Depropagation Kinetics of Sterically Demanding Monomers: A Pulsed Laser Size Exclusion Chromatography Study. *Macromolecules* **2005**, *38*, 5944–5954. [CrossRef]
27. Penelle, J.; Collot, J.; Rufflard, G. Kinetic and thermodynamic analysis of methyl ethacrylate radical polymerization. *J. Polym. Sci.* **1993**, *31*, 2407–2412. [CrossRef]
28. Brandrup, J.; Immergut, E.; Grulke, E. *Polymer Handbook*, 4th ed.; John Wiley & Sons: New York, NY, USA, 1999; ISBN 978-0-471-47936-9.
29. Morris, L.; Davis, T.; Chaplin, R. Radical copolymerization propagation kinetics of methyl ethacrylate and styrene. *Polymer* **2001**, *42*, 941–952. [CrossRef]
30. Ueda, M.; Takahashi, M.; Imai, Y.; Pittman, C.U. Synthesis and homopolymerization kinetics of α-methylene-δ-valerolactone, an exo-methylene cyclic monomer with a nonplanar ring system spanning the radical center. *Macromolecules* **1983**, *16*, 1300–1305. [CrossRef]
31. Drawe, P.; Buback, M.; Lacík, I. Radical Polymerization of Alkali Acrylates in Aqueous Solution. *Macromol. Chem. Phys.* **2015**, *216*, 1333–1340. [CrossRef]
32. Drawe, P. Kinetic of the Radical Polymerization of Ionic Monomers in Aqueous Solution: Spectroscopic Analysis and Modelling. Ph.D. Thesis, University of Göttingen, Göttingen, Germany, 2016.

33. Barth, J.; Buback, M. SP-PLP-EPR Study into the Termination Kinetics of Methacrylic Acid Radical Polymerization in Aqueous Solution. *Macromolecules* **2011**, *44*, 1292–1297. [CrossRef]
34. Wulkow, M. Computer Aided Modeling of Polymer Reaction Engineering—The Status of Predici, 1—Simulation. *Macromol. React. Eng.* **2008**, *2*, 461–494. [CrossRef]
35. Wittenburg, N. Kinetics and Modeling of the Radical Polymerization of Acrylic Acid and of Methacrylic Acid in Aqueous Solution. Ph.D. Thesis, University of Göttingen, Göttingen, Germany, 2013.
36. Wako Pure Chemical Industries Ltd. "V-50". Available online: http://www.wako-chem.co.jp/kaseihin_en/waterazo/V-50.htm (accessed on 31 March 2017).
37. Wako Pure Chemical Industries Ltd. "VA-086". Available online: http://www.wako-chem.co.jp/kaseihin_en/waterazo/VA-086.htm (accessed on 31 March 2017).
38. Barth, J.; Buback, M. Termination and Transfer Kinetics of Sodium Acrylate Polymerization. *Macromolecules* **2012**, *45*, 4152–4157. [CrossRef]
39. Luk, S.B. Radical Polymerization Kinetics of Bio-Renewable Monomers in Aqueous Solution. Master's Thesis, Queen's University, Kingston, ON, Canada, 2017.
40. Kattner, H.; Drawe, P.; Buback, M. Chain-Length-Dependent Termination of Sodium Methacrylate Polymerization in Aqueous Solution Studied by SP-PLP-EPR. *Macromolecules* **2017**, *50*, 1386–1393. [CrossRef]
41. Kattner, H.; Buback, M. Termination and Transfer Kinetics of Acrylamide Homopolymerization in Aqueous Solution. *Macromolecules* **2015**, *48*, 7410–7419. [CrossRef]